Supporting Information for

The binuclear cluster of [FeFe] hydrogenase is formed with sulfur donated by cysteine of an [Fe(Cys)(CO)$_2$(CN)] organometallic precursor

Guodong Rao[a,1], Scott A. Pattenaude[b,1], Katherine Alwan[c], Ninian J. Blackburn[c], R. David Britt[a,2]*, Thomas B. Rauchfuss[b,2]*

[a]Department of Chemistry, University of California, Davis, CA 95616; [b]School of Chemical Sciences, University of Illinois at Urbana-Champaign, Urbana, IL 61801; [c]Department of Chemical Physiology and Biochemistry, Oregon Health and Science University, Portland, OR 97239.

[1]G.R. and S.A.P. contributed equally to this work.

[2]To whom correspondence may be addressed. Email: rauchfuz@illinois.edu or rdbritt@ucdavis.edu.

www.pnas.org/cgi/doi/10.1073/pnas.1913324116

Methods

General Considerations. All chemical syntheses were conducted under a nitrogen atmosphere in an Mbraun glovebox. Methanol and acetonitrile were dried and deoxygenated using literature procedures with a Seca solvent purification system.(1) L-cysteine and cysteamine were purchased from Sigma-Aldrich and used without further purification. $K^{13}CN$ and L-cysteine-$^{13}C_3$,^{15}N were purchased from Cambridge Isotope Laboratories and used without further purification.

Preparation of $[Et_4N][FeI_2(CN)(CO)_3]$. In the dark, a 20 mL scintillation vial was charged with 50 mg (0.154 mmol) of $[Et_4N][Fe(CN)(CO)_4]$ and 5 mL of dry MeOH (or CH_3CN). A solution of 39 mg (0.154 mmol) of I_2 in 5 mL of MeOH (or CH_3CN) was added dropwise over the course of 5 minutes, resulting in gas evolution and a color change from yellow to orange. After stirring for 30 minutes, the solution was concentrated *in vacuo* to an orange solid assigned as $[Et_4N][FeI_2(CN)(CO)_3]$ (0.081 g, 0.148 mmol, 96%). IR (MeOH, v/cm^{-1}): 2123 w (ν_{CN}), 2092 m (ν_{CO}), 2051 s (ν_{CO}), 2032 sh (ν_{CO}). IR (CH_3CN, v/cm^{-1}): 2122 w (ν_{CN}), 2091 m (ν_{CO}), 2047 s (ν_{CO}), 2030 sh (ν_{CO}). MS (ESI): *m/z* = 419.5 $[M]^-$, 335.5 $[M - 3(CO)]^-$. Analysis for $C_{12}H_{20}FeI_2N_2O_3$: Calcd. C, 26.21; H, 3.67; N, 5.09; I, 46.15. Found C, 25.71; H, 4.04; N, 5.90; I, 48.83. Note: Elemental analysis is consistent with a small degree of decarbonylation upon analysis (elevated hydrogen, nitrogen, and iodine values; lower than expected carbon value). For this reason, *in situ* generation of $[Et_4N][FeI_2(CN)(CO)_3]$ is preferred over using isolated material.

Preparation of syn-B. In the dark, a 20 mL scintillation vial was charged with 50 mg (0.154 mmol) of $[Et_4N][Fe(CN)(CO)_4]$ and 5 mL of dry MeOH. A solution of 39 mg (0.154 mmol) of I_2 in 5 mL of MeOH was added dropwise over the course of 5 minutes, resulting in gas evolution and a color change from yellow to orange. Monitoring these reaction mixtures by IR indicates that this oxidation is complete within the first few minutes of iodine addition. The spectrum (IR (MeOH, v/cm^{-1}): 2123 w (ν_{CN}), 2092 m (ν_{CO}), 2051 s (ν_{CO}), 2032 sh (ν_{CO})) was assigned to the formation of $[Et_4N][FeI_2(CN)(CO)_3]$, with similar shifts to other $[FeI_2(CN)(CO)_3]^-$ salts in the literature.(2, 3) In a separate vial, 19 mg (0.157 mmol) of L-cysteine and 17 mg (0.302 mmol) KOH were combined in 5 mL of MeOH. After stirring for approximately 5 minutes, the L-cysteine was solubilized, generating a clear, colorless solution. At this point, this cysteinate solution was added dropwise to the iron-containing solution over the course of 5 minutes, resulting in a light orange, homogenous solution. After stirring for one hour, this solution was concentrated *in vacuo*, resulting in an orange-brown solid. This solid was washed with acetone (4 x 50 mL) to remove KI, leaving

a light orange-brown solid (52 mg) designated as **syn-B**. IR (MeOH, v/cm^{-1}): 2111 w (ν_{CN}), 2046 s (ν_{CO}), 1993 s (ν_{CO}), 1615 br (ν_{COO-}). IR (H_2O, v/cm^{-1}): 2107 w (ν_{CN}), 2058 s (ν_{CO}), 2010 s (ν_{CO}). IR (D_2O, v/cm^{-1}): 2106 w (ν_{CN}), 2057 s (ν_{CO}), 2009 s (ν_{CO}), 1603 br (ν_{COO-}). MS (ESI): *m/z* = 201.0 [Fe(cys)(CN)]$^-$. Analysis for $C_{56}H_{108}Fe_5I_2N_{12}O_{20}S_4$: Calculated C, 34.84; H, 5.64; N, 8.71; I, 13.15. Found: C, 33.82; H, 6.61; N, 6.42; I, 14.34. Note: the concentration and rate of reagent addition of this reaction is important. The reaction is unsuccessful if conducted under more concentrated conditions.

Preparation of syn-B-^{13}CN. In the dark, a 20 mL scintillation vial was charged with 100 mg (0.237 mmol) of $FeI_2(CO)_4$ and 10 mL of dry MeOH. A solution of 16 mg (0.242 mmol) of K^{13}CN in 5 mL of MeOH was added dropwise over the course of 5 minutes, resulting in gas evolution and a color change from yellow to dark-orange, with a small amount of precipitate. In a separate vial, 29 mg (0.239 mmol) of L-cysteine and 27 mg (0.481 mmol) KOH were combined in 5 mL of MeOH. After stirring for approximately 5 minutes, the L-cysteine was solubilized, generating a clear, colorless solution. At this point, this cysteinate solution was added dropwise to the iron-containing solution over the course of 5 minutes, resulting in a light orange solution. After stirring for one hour, this solution was filtered and concentrated *in vacuo*, resulting in an orange-brown solid. This solid was washed with acetone (4 x 50 mL) to remove KI, leaving a light orange-brown solid (76 mg) designated as **syn-B-^{13}CN**. IR (MeOH, v/cm^{-1}): 2080 w (ν_{CN}), 2037 s (ν_{CO}), 1994 s (ν_{CO}), 1608 br (ν_{COO-}). IR (H_2O, v/cm^{-1}): 2074 w (ν_{CN}), 2047 s (ν_{CO}), 2010 s (ν_{CO}). MS (ESI): *m/z* = 201.9 [Fe(cys)(^{13}CN)]$^-$.

Preparation of syn-B-$^{13}C_3$,^{15}N. In the dark, a 20 mL scintillation vial was charged with 50 mg (0.154 mmol) of $[Et_4N][Fe(CN)(CO)_4]$ and 5 mL of dry MeOH. A solution of 39 mg (0.154 mmol) of I_2 in 5 mL of MeOH was added dropwise over the course of 5 minutes, resulting in gas evolution and a color change from yellow to orange. In a separate vial, 19 mg (0.152 mmol) of L-cysteine-$^{13}C_3$,^{15}N and 17 mg (0.302 mmol) KOH were combined in 5 mL of MeOH. After stirring for approximately 5 minutes, the L-cysteine was solubilized, generating a clear, colorless solution. At this point, this cysteinate solution was added dropwise to the iron-containing solution over the course of 5 minutes, resulting in a light orange, homogenous solution. After stirring for one hour, this solution was concentrated *in vacuo*, resulting in an orange-brown solid. This solid was washed with acetone (4 x 50 mL) to remove KI, leaving a light orange-brown solid (49 mg) designated as **syn-B-$^{13}C_3$,^{15}N**. IR (MeOH, v/cm^{-1}): 2111 w (ν_{CN}), 2046 s (ν_{CO}), 1994 s (ν_{CO}), 1575 br (ν_{COO-}). MS (ESI): *m/z* = 205.0 [Fe($^{13}C_3$,^{15}N-cys)(CN)]$^-$. Note: the concentration and rate of

reagent addition of this reaction is important. The reaction is unsuccessful if conducted under more concentrated conditions.

Preparation of syn-B-cysam. In the dark, a 20 mL scintillation vial was charged with 50 mg (0.154 mmol) of $[Et_4N][Fe(CN)(CO)_4]$ and 5 mL of dry MeOH. A solution of 39 mg (0.154 mmol) of I_2 in 5 mL of MeOH was added dropwise over the course of 5 minutes, resulting in gas evolution and a color change from yellow to orange. In a separate vial, 12 mg (0.156 mmol) of cysteamine and 9 mg (0.160 mmol) KOH were combined in 5 mL of MeOH. After stirring for approximately 2 minutes the cysteamine solution was added dropwise to the iron-containing solution over the course of 5 minutes, resulting in a light orange, homogenous solution. After stirring for one hour, this solution was concentrated *in vacuo*, resulting in an orange-brown solid. This solid was washed with acetone (4 x 50 mL) to remove KI, leaving a light orange-brown solid (35 mg) designated as **syn-B-cysam**. IR (MeOH, v/cm^{-1}): 2106 w (ν_{CN}), 2043 s (ν_{CO}), 1992 s (ν_{CO}). IR (H_2O, v/cm^{-1}): 2098 w (ν_{CN}), 2053 s (ν_{CO}), 2007 s (ν_{CO}). Analysis for $C_{44}H_{84}Fe_5I_5N_{11}O_8S_4$: Calculated C, 27.28; H, 4.37; N, 7.95; I, 32.75. Found: C, 26.99; H, 4.29; N, 6.10; I, 32.40.

Preparation of syn-B-Secys. In the dark, a 20 mL scintillation vial was charged with 50 mg (0.154 mmol) of $[Et_4N][Fe(CN)(CO)_4]$ and 5 mL of dry MeOH. A solution of 39 mg (0.154 mmol) of I_2 in 5 mL of MeOH was added dropwise over the course of 5 minutes, resulting in gas evolution and a color change from yellow to orange. In a separate vial, 26 mg (0.078 mmol) of L-selenocystine and 9 mg (0.160 mmol) KOH were combined in 5 mL of MeOH. After stirring for approximately 10 minutes, the selenocystine was solubilized, generating a clear, yellow solution. A solution of 6 mg (0.158 mmol) of sodium borohydride in 5 mL of MeOH was added to the selenocystine solution resulting in a clear, colorless solution after 30 minutes of stirring. At this point, this selenocysteinate solution was added dropwise to the iron-containing solution over the course of 5 minutes, resulting in a light orange, homogenous solution. After stirring for one hour, this solution was concentrated *in vacuo*, resulting in an orange-brown solid. This solid was washed with acetone (4 x 50 mL) to remove salts, leaving a light orange-brown solid (55 mg) designated as **syn-B-Secys**. IR (MeOH, v/cm^{-1}): 2109 w (ν_{CN}), 2040 s (ν_{CO}), 1988 s (ν_{CO}), 1624 br (ν_{COO-}). IR (H_2O, v/cm^{-1}): 2102 w (ν_{CN}), 2049 s (ν_{CO}), 2006 s (ν_{CO}). MS (ESI): *m/z* = 304.8 [Fe(Se-cys)(CN)$(CO)_2]^-$, 248.8 [Fe(Se-cys)(CN)]$^-$.

Maturation of *Cr*HydA1. Expression and purification of apo-*Cr*HydA1, expression and preparation of HydE, HydF, and HydG lysate, and maturation of *Cr*HydA1 using cell lysate followed previous procedures.(4, 5) For maturation with **syn-B**, HydG cell lysate and Tyr are omitted from the recipe. Instead, 150 µM **syn-B** (based on the formula

$(Et_4N)_4\{FeI_2[Fe(Cys)(CN)(CO)_2(H_2O)]_4\}$, or 600 μM based on $[Fe(Cys)(CO)_2(CN)]$ unit) was supplemented into the reaction mixture. The maturation reaction was performed for 3 hours when using **syn-B**.

EPR spectroscopy. EPR spectroscopy was performed in the CalEPR center in Department of Chemistry, University of California at Davis. X-band (9.4 GHz) Continuous Wave (CW) EPR spectra were recorded on a Bruker Biospin EleXsys E500 spectrometer equipped with a super high Q resonator (ER4122SHQE). Cryogenic temperatures were achieved and controlled by using an ESR900 liquid helium cryostat, a temperature controller (Oxford Instrument ITC503) and a gas flow controller. Pulse X-band (34 GHz) hyperfine sublevel correlation (HYSCORE) and Q-band Davies electron nuclear double resonance (ENDOR) experiments were performed on the Bruker Biospin EleXsys 580 spectrometer using a split ring MS5 resonator and a R.A. Isaacson cylindrical TE_{011} resonator, respectively.(6) Cryogenic temperatures were achieved and controlled with an Oxford Instrument CF935 cryostat. The pulse sequences employed were as follows: HYSCORE ($\pi/2$-τ-$\pi/2$-t_1-π-t_2-$\pi/2$-τ-echo), Davies-ENDOR (π-RF-$\pi/2$-τ-π-τ-echo). EPR spectral simulations were performed in Matlab 2014a (MathWorks, Inc,) with EasySpin 5.2.13 toolbox.(7)

H_2 production assay. H_2 production assay were performed according to previous procedures.(8) Briefly, the reaction mixture contained 10 nM HydA1 and 5 mM methyl viologen in 3 mL pH = 6.8 phosphate buffer in a 15 mL sealed tube under N_2 atmosphere. The reaction was initiated by injecting 30 μL 1 M freshly made sodium dithionite and was continued for ~40 min. H_2 production was monitored by injecting 500 μL headspace every 5 min into a Varian 3800 gas chromatography equipped with a 60/80 Å molecular sieve and the thermal conductivity detector.

Pyruvate analysis. Two maturation reactions, one using **syn-B** and the other using **syn-B-$^{13}C_3$,^{15}N,** were performed for 30 min before they were quenched by freezing. For the analysis of each sample, 100 μL of solution was dried under vacuum and derivatized with 50 μL methoxyamine hydrochloride (Sigma-Aldrich, MO, USA) (40 mg/ml in pyridine) for 60 minutes at 50 °C, then with 50 μL MSTFA+1%TMCS (Thermo, MA, USA) at 70 °C for 120 minutes. This was followed with a 2-hour incubation at room temperature. Chromatograms were acquired using a GC-MS system (Agilent Inc, CA, USA) consisting of an Agilent 7890 gas chromatograph, an Agilent 5975 MSD, and a HP 7683B autosampler. Gas chromatography was performed on a ZB-5MS (60m×0.32mm I.D. and 0.25μm film thickness) capillary column (Phenomenex, CA, USA). The inlet and MS interface temperatures were 250 ˚C, and the ion source temperature was adjusted to 230 ˚C. An aliquot of 1 μL was injected with the split ratio of 10:1. The helium carrier gas was kept at a constant flow rate of 2 mL/min. The temperature program was: 5-min isothermal

heating at 70 ˚C, followed by an oven temperature increase of 5 ˚C min^{-1} to 310 ˚C and a final 10 min at 310 ˚C. The mass spectrometer was operated in positive electron impact mode (EI) at 69.9 eV ionization energy at m/z 30-800 scan range. Target peaks were evaluated by the Mass Hunter Quantitative Analysis B.08.00 (Agilent Inc., CA, USA) software. Calibration curve was built for 700 – 3.5 uM concentration range. The instrument variability was within the standard acceptance limit (5%).

XAS spectroscopy. Fe K (7111 eV) and Se K (12658 eV) X-ray absorption fine structure (EXAFS) and X-ray absorption near edge structure (XANES) were collected on beam lines 7.3 and 9.3 at the Stanford Synchrotron Radiation Lightsource (SSRL). The data shown in the manuscript were measured on BL 9.3 with the ring operating at 500 mA in continuous top-up mode. To avoid detector saturation and other non-linear effects that generate discontinuities in the F/I_0 ratios, the beam was defocused approximately 50 percent to a beam size of 5 x 1 mm. BL 9.3 was configured with a Si [220] monochromator and Rd-coated mirror upstream of the monochromator to reject harmonics set to an energy cut-off of 10 kEV for measurements at the Fe edge and 15 keV for measurements at the Se edge. On BL 7.3, harmonic rejection was achieved by detuning the mono by 20 per cent. Energy calibration was achieved by simultaneous measurement of a metal calibration foil placed between the second and third ionization chambers. The first inflexion points of the metal spectra were used to calibrate the monochromator to 7111.0 eV for Fe, and 12658.0 eV for Se. Canberra 30-element (BL 7.3) or 100-element (BL 9.3) fluorescent detectors were used to collect the Se and Fe x-ray fluorescence positioned at 90° to the beam. A Soller slit assembly fitted with Z-1 metal oxide filters was used to reduce the elastic scatter peak.

Samples were measured as aqueous glasses in 20 % ethylene glycol at 10 K with temperature control provided by a liquid He cryostat (Oxford Instruments). Two scans were collected at each edge and averaged to increase the signal to noise. For Se, two scans of a buffer blank were also collected and subtracted from the raw data to remove the curvature of the pre-edge and arsenic Kβ fluorescence arising from the Z-1 filter, but for Fe, the pre-edge was flat and did not require blank subtraction. Data reduction and background subtractions were performed using the program modules of EXAFSPAK (9). Output from each detector channel was inspected for glitches and dropouts before inclusion in the final average. Spectral simulation was carried out using EXCURVE version 9.2(10) as described previously(11, 12). For Fe edge simulations a mixed-shell model was utilized consisting of S/Se from inorganic sulfide or Cys/SeCys coordination, CO and CN from carbonyl/cyanide ligands, and second shell Fe-Fe interactions. Se data were simulated using Se-C and Se-Fe interactions. The threshold energy, E0, was chosen

at 7116 eV for Fe, and 12663eV for Se. Parameters floated in the fits included distances (R), coordination numbers (N, integer values only), and Debye-Waller factors ($2\sigma^2$), and included multiple scattering contributions from outer-shell atoms of linear CO and CN groups. Since the latter are isostructural, they were simulated by a single shell of CO.

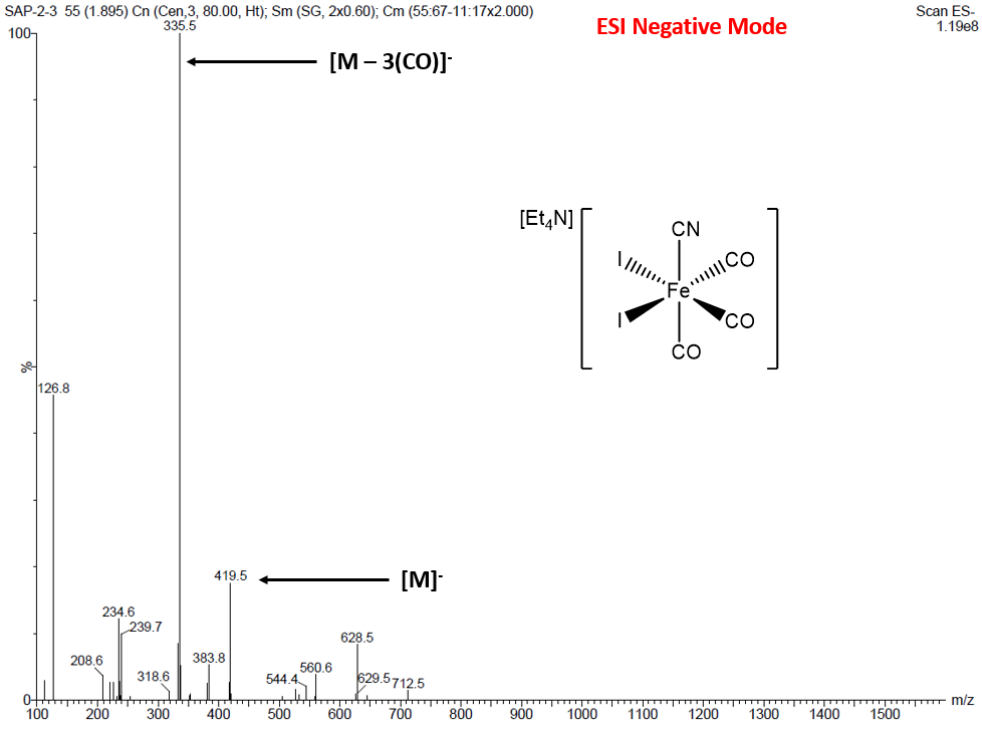

Figure S1. Mass spectrum (ESI; Negative Mode) of $[Et_4N][FeI_2(CN)(CO)_3]$.

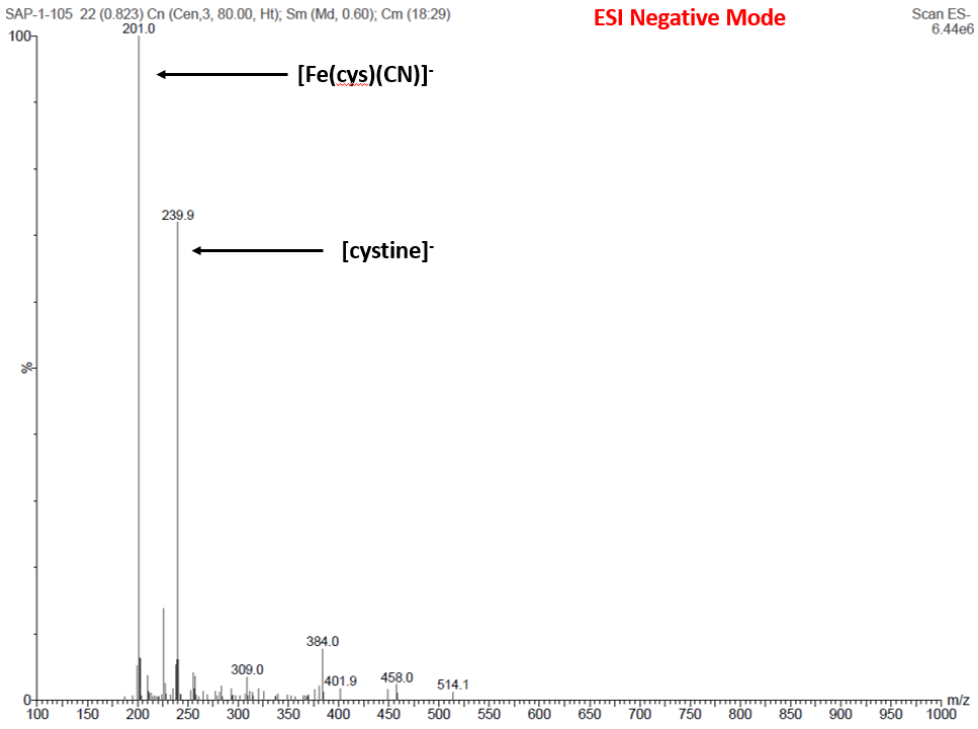

Figure S2. Mass spectrum (ESI; Negative Mode) of **syn-B**.

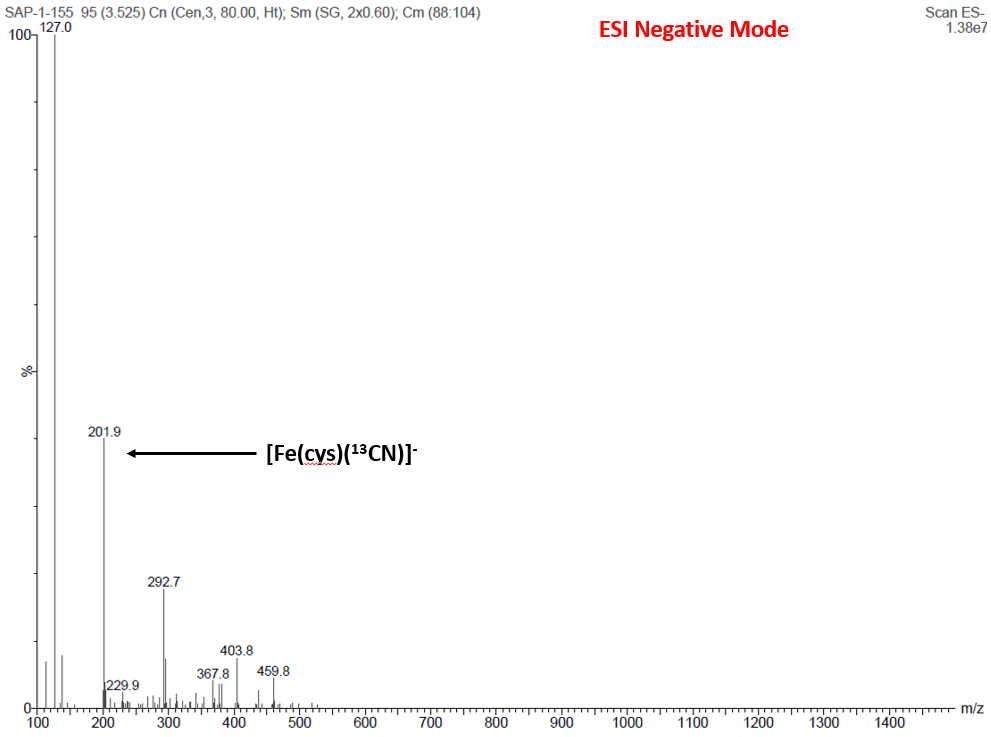

Figure S3. Mass spectrum (ESI; Negative Mode) of **syn-B-^{13}CN**.

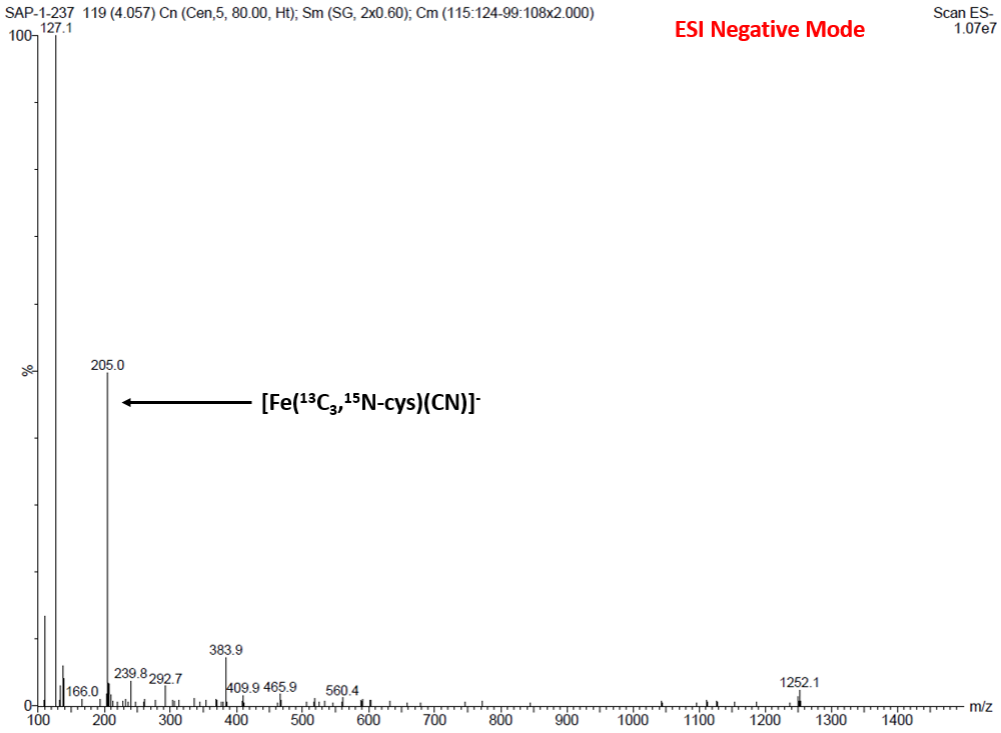

Figure S4. Mass spectrum (ESI; Negative Mode) of **syn-B-$^{13}C_3$,^{15}N**.

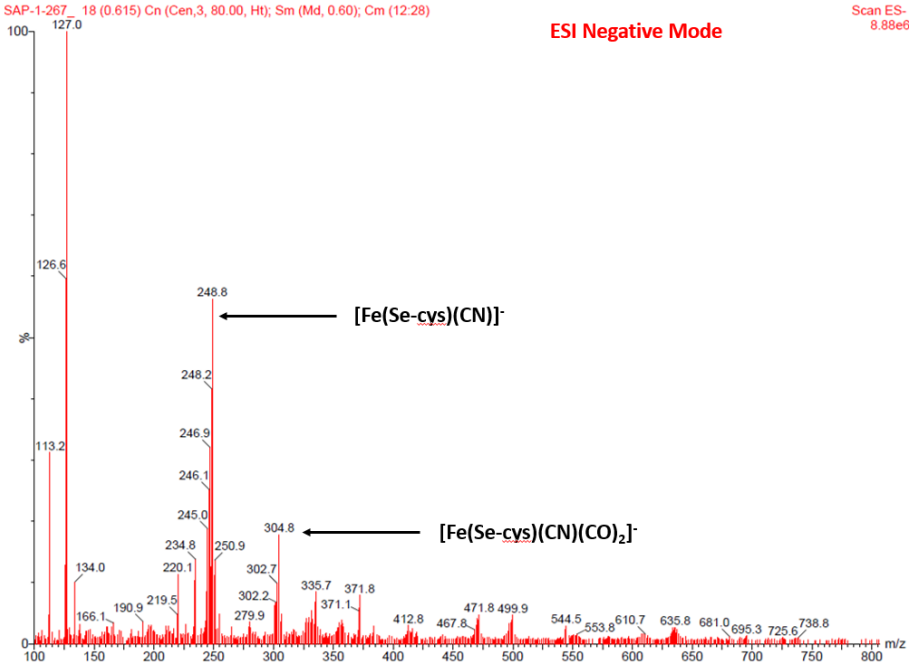

Figure S5. Mass spectrum (ESI; Negative Mode) of **syn-B-Secys**.

Table S1. Summary of the IR frequencies of syn-B analogues synthesized in this study and Complex B.

	in H_2O			in MeOH		
	ν_{CN} (cm^{-1})	ν_{CO} (cm^{-1})	ν_{CO} (cm^{-1})	ν_{CN} (cm^{-1})	ν_{CO} (cm^{-1})	ν_{CO} (cm^{-1})
Complex B	2105	2057	2006	-	-	-
syn-B	2107	2058	2010	2111	2046	1993
syn-B-^{13}CN	2074	2047	2010	2080	2037	1994
syn-B-$^{13}C_3$,^{15}N	-	-	-	2111	2046	1994
syn-B-Secys	2102	2049	2006	2109	2040	1988
syn-B-cysam	2098	2053	2007	2106	2043	1992

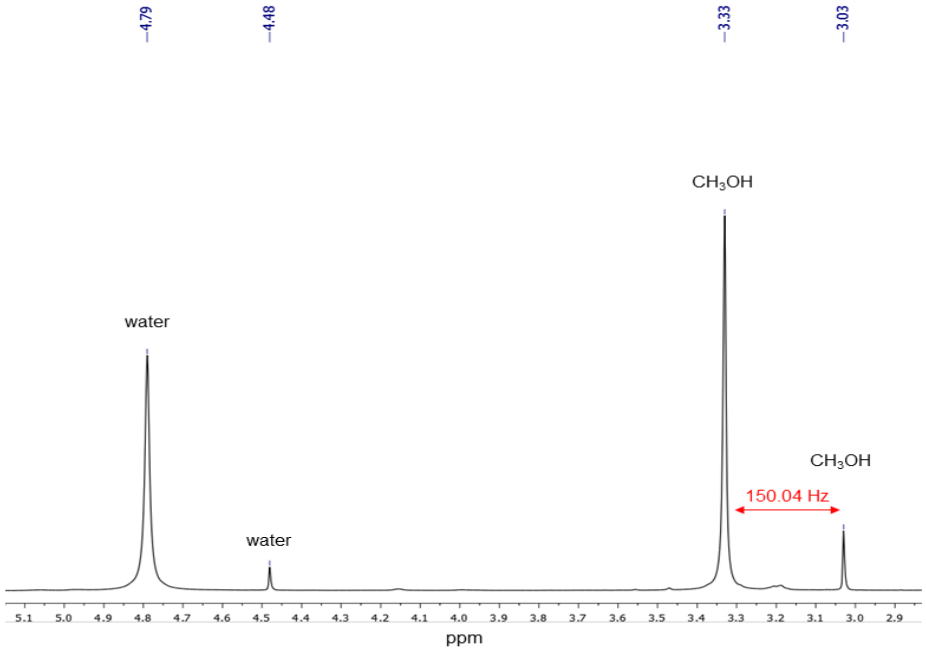

Figure S6. ^{1}H NMR Evan's method analysis of **syn-B**. Sample contains 31 mg **syn-B** and 2.125 g D_2O. Instrument was operating at 499.43 MHz and 293.15 K. Added methanol was used for a standard.

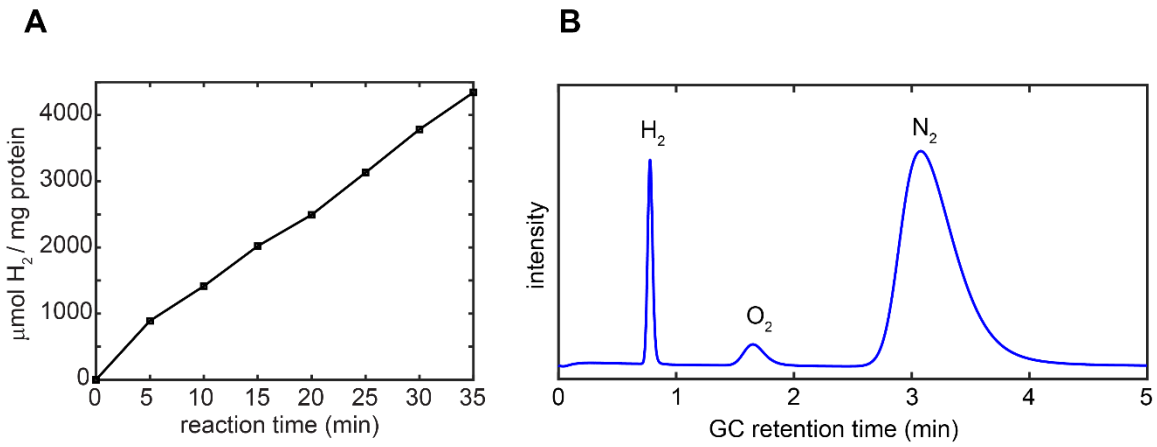

Figure S7. (A) The time course of H_2 production by [**syn-B**]-*Cr*HydA1. (B) Typical GC trace of the headspace of the 40 min reaction sample.

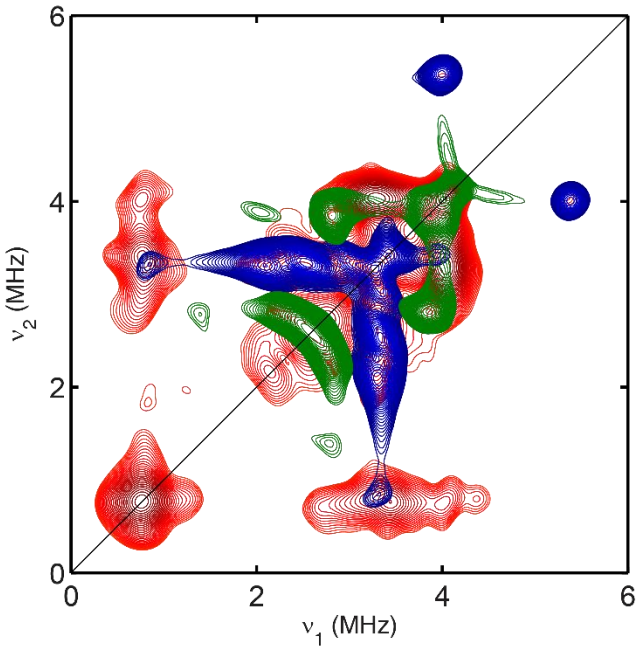

Figure S8. Simulation of the HYSCORE spectra in Figure 4 using the ^{14}N hyperfine tensors previously reported.(13) Red contour: experimental data. Blue contour: simulation of adt ^{14}N using g = [2.103, 2.042, 1.998], A (^{14}N) = [1.35, 1.15, 1.15] MHz, Euler angle = [0, 0, 0]°, e^2Qq/h (^{14}N) = 4.92 MHz, η = 0.13, Euler angle = [0, 90, 0]°. Green contour: simulation of distal CN ^{14}N using g = [2.103, 2.042, 1.998], A (^{14}N) = [-0.9, -0.8, 4.2] MHz, Euler angle = [0, 45, 90]°, e^2Qq/h (^{14}N) = 3.60 MHz, η = 0.34, Euler angle = [0, 90, 0]°.

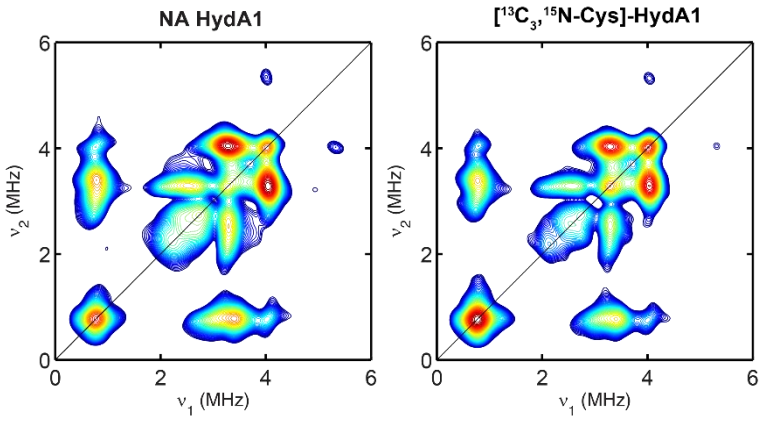

Figure S9. Comparison of X-band HYSCORE spectra collected at *g* = 2.103 of native holo-*Cr*HydA1 and *Cr*HydA1 maturated wih $^{13}C_3$,^{15}N-Cys supplemented into the maturation reaction. Spectrometer settings are indicated in Figure 4.

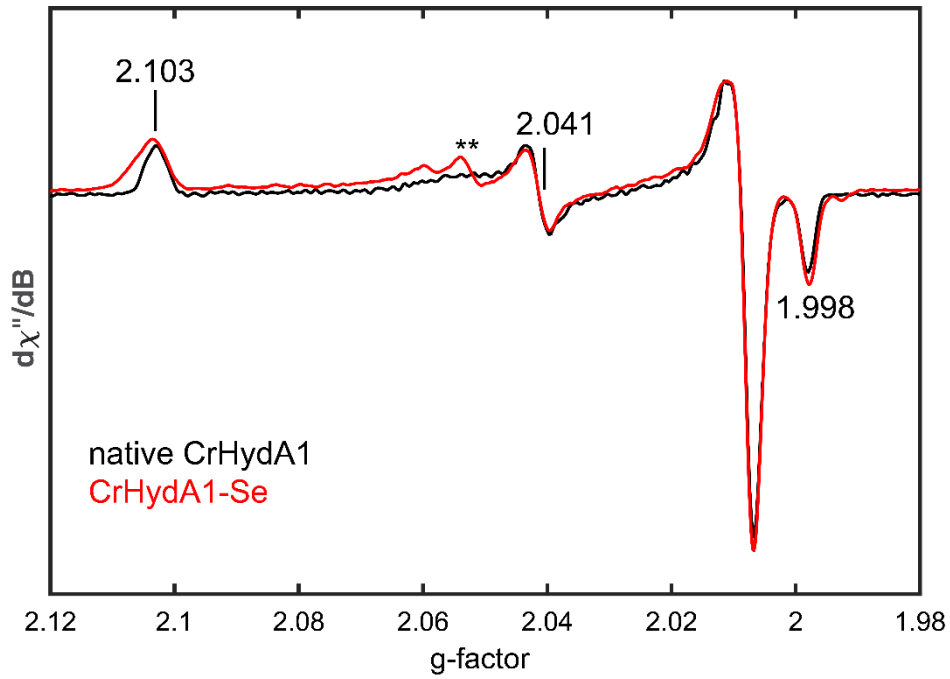

Figure S10. Comparison of the Q-band pseudomodulated echo-detected EPR spectra of native *Cr*HydA1 and *Cr*HydA1 maturated from **syn-B-Secys**. Both samples were poised in the H_{ox} state by adding 2 mM thionine. EPR conditions: temperature, 15 K; τ, 300 ns. The EPR feature denoted with ** is an impurity.

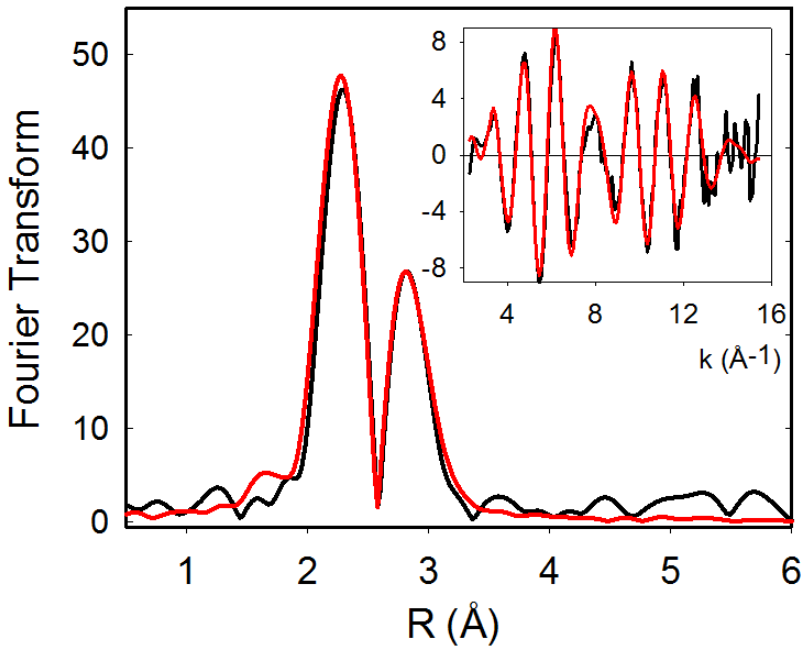

Figure S11. Fourier transforms and EXAFS (insets) for the Fe K edges of native *Cr*HydA1. Black traces are experimental data. Red traces are simulated using parameters listed in Table S1.

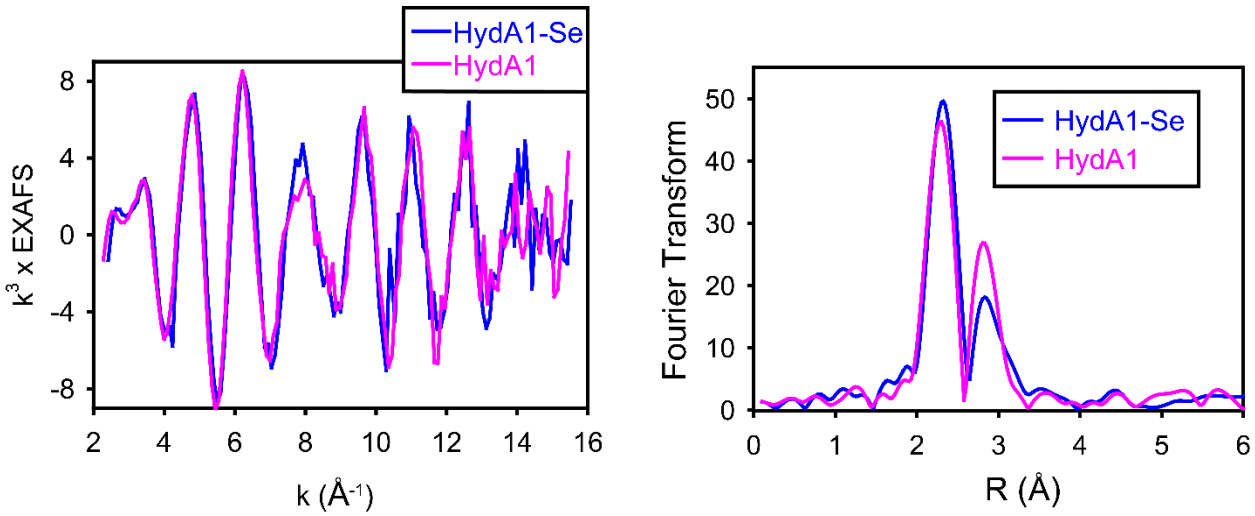

Figure S12. Comparison of the Fe K-edge EXAFS (left) and Fourier transforms (right) of the native and Se-labeled *Cr*HydA1.

Table S2. Fits obtained to the Se and Fe K-edge EXAFS derivatives of *Cr*HydA1. For the Fe data, the EXAFS are simulated assuming a structure for the H cluster as depicted by crystallography, including Fe_4S_4 and Fe-Fe sub-clusters. Shell occupancies of the Fe ligands correspond to the total number of Fe-X interactions expected in the cluster divided by the number of Fe atoms (6)

Shell	Assignment	F[a]	No[b]	R (Å)[c]	DW (Å²)[d]	-ΔE₀
Selenium						
Se-C	Se-adt	1.34	1	1.96	0.0150	3.23
Se-Fe[g]	Se-adt-Fe		2	2.43	0.0065	
Iron-SeCys						
Fe-S	FeS cluster	1.08	3	2.29	0.0090	5.3
Fe-Se	Fe-Se-adt		0.7	2.43	0.0061	
Fe-CO/CN[e]	CO/CN ligands		1	1.78	0.0090	
Fe-Fe	Fe-Fe subcluster FeS cluster		3	2.72	0.0220	
Iron S-Cys						
Fe-S	FeS cluster + S-adt	1.03	3.7	2.30	0.0090	7.7
Fe-CO/CN[e]	CO/CN ligands		1	1.76	0.0090	
Fe-Fe	Fe-Fe subcluster FeS cluster		3	2.74	0.0120	

[a] F is a least-squares fitting parameter defined as $F^2 = \frac{1}{N}\sum_{i=1}^{N} k^6 (Data - Model)^2$

[b] Coordination numbers are generally considered accurate to ± 25% except where indicated as low confidence.

[c] In any one fit, the statistical error in bond-lengths is ±0.005 Å. However, when errors due to imperfect background subtraction, phase-shift calculations, and noise in the data are compounded, the actual error is probably closer to ±0.02 Å.

[d] Debye Waller terms (DW) are reported as $2\sigma^2$ (Å²), and correspond to twice the mean square deviation of the bond distance from the simulated value.

[e] Fits included both single and multiple scattering contributions from the linear CO and CN ligands. Position of the O and N atoms indicate average C≡O and C≡N bond lengths of 1.05(5) Å, and ∠Fe-C-O/N =180(10)°.

References

1. A. B. Pangborn, M. A. Giardello, R. H. Grubbs, R. K. Rosen, F. J. Timmers, Safe and Convenient Procedure for Solvent Purification. *Organometallics* **15**, 1518-1520 (1996).
2. A. Stock *et al.*, Synthesis of fac-$[Fe^{II}(CN)(CO)_3I_2]^-$ and chemistry of the fac-$[Fe^{II}(CN)_x(CO)_3I_{(3-x)}]^-$ series (x=1–3). *Inorg. Chem. Commun.* **18**, 105-109 (2012).
3. W.-F. Liaw *et al.*, Dinuclear Iron(II)−Cyanocarbonyl Complexes Linked by Two/Three Bridging Ethylthiolates: Relevance to the Active Site of [Fe] Hydrogenases. *Inorg. Chem.* **42**, 2783-2788 (2003).
4. J. M. Kuchenreuther, S. A. Shiigi, J. R. Swartz, Cell-free synthesis of the H-cluster: a model for the in vitro assembly of metalloprotein metal centers. *Methods Mol. Biol.* **1122**, 49-72 (2014).
5. G. Rao, R. D. Britt, Electronic structure of two catalytic states of the [FeFe] hydrogenase H-cluster as probed by pulse electron paramagnetic resonance spectroscopy. *Inorg. Chem.* **57**, 10935-10944 (2018).
6. R. Calvo *et al.*, EPR study of the molecular and electronic structure of the semiquinone biradical Q_a^{-}•Q_b^{-}• in photosynthetic reaction centers from *Rhodobacter sphaeroides*. *J. Am. Chem. Soc.* **122**, 7327-7341 (2000).
7. S. Stoll, A. Schweiger, EasySpin, a comprehensive software package for spectral simulation and analysis in EPR. *J. Magn. Reson.* **178**, 42-55 (2006).
8. G. Berggren *et al.*, Biomimetic assembly and activation of [FeFe]-hydrogenases. *Nature* **499**, 66-69 (2013).
9. G. N. George (1995) EXAFSPAK. (Stanford Synchrotron Radiation Laboratory, Menlo Park, CA).
10. N. Binsted, S. J. Gurman, J. W. Campbell (1998) EXCURVE. (Daresbury Laboratory, Warrington, England).
11. K. N. Chacon, N. J. Blackburn, Stable Cu(II) and Cu(I) Mononuclear Intermediates in the Assembly of the CuA Center of Thermus thermophilus Cytochrome Oxidase. *J. Am. Chem. Soc.* **134**, 16401-16412 (2012).
12. K. N. Chacon, T. D. Mealman, M. M. McEvoy, N. J. Blackburn, Tracking metal ions through a Cu/Ag efflux pump assigns the functional roles of the periplasmic proteins. *Proc. Natl. Acad. Sci. U S A* **111**, 15373-15378 (2014).
13. A. Adamska-Venkatesh *et al.*, Spectroscopic characterization of the bridging amine in the active site of [FeFe] hydrogenase using isotopologues of the H-cluster. *J. Am. Chem. Soc.* **137**, 12744-12747 (2015).